Transverse instabilities and pattern formation in two-beam-excited nonlinear optical interactions in liquids

Sean J. Bentley,* John E. Heebner,† and Robert W. Boyd

The Institute of Optics, University of Rochester, Rochester, New York 14627

Received October 17, 2005; revised December 21, 2005; accepted December 25, 2005; posted January 9, 2006 (Doc. ID 65434)

We describe observations of various transverse instabilities that occur when two laser beams intersect in nonlinear optical liquids. Patterns that we observe include two types of conical emission and the generation of a linear array of spots. These results can be understood in terms of the physical processes of self-diffraction, two-beam-excited conical emission, and seeded modulational instability. © 2006 Optical Society of America

OCIS codes: 190.4420, 190.4380.

Various transverse instabilities can occur when laser beams propagate through a nonlinear optical medium. The understanding of these instabilities is important because, on the one hand, they limit the total optical power that can be transmitted through a given material and, on the other hand, they can lead to useful processes such as soliton formation. Examples of transverse instabilities include self-diffraction,[1–4] seeded conical modulational instability,[5–9] and two-beam-excited conical emission (TBECE).[10,11] A detailed theoretical treatment of some of these processes and their interplay has been performed by Kauranen *et al.*[12] Much of the prior work in this area has made use of the nonlinear response of atomic vapors.[13,14] In the present work we study these instabilities for the case of liquid media, which hold particular promise for certain applications because of their shorter response times.

The experimental configuration used in our studies is shown in Fig. 1. The second-harmonic output (at 532 nm) of a 25 ps, 10 Hz Nd:YAG laser is used. A half-wave plate (HWP) and a polarizing beam splitter (PBS) are used to divide the laser output into two beams with controllable power ratios. A second HWP is used to control the relative polarizations of the two beams. A polarization-insensitive beam splitter is then used to direct the two beams into a cell containing the nonlinear liquid. The system is aligned such that the two pulses overlap in space and time within the cell. The output of the cell is then imaged onto an observation screen. The beam intensities are monitored using the other output port of the second beam splitter.

We found that the beam crossing angle is a crucial parameter in determining the structure of the generated patterns. For small crossing angles (of the order of a few mrad), a linear array of spots is observed, as shown in Fig. 2. We describe this process by means of the nonlinear Schrödinger equation[15]

$$\partial A/\partial z = (i/2k_o)\nabla_\perp^2 A + i\gamma|A|^2 A, \qquad (1)$$

where A is the slowly varying envelope of the optical field and γ is a measure of the nonlinearity given by $\gamma \equiv n_0 n_2 \omega_0 / 2\pi$, where n_0 and n_2 are the linear and nonlinear refractive indices, respectively, and ω_0 is the optical frequency. The field amplitude A in this equation represents the total optical field within the nonlinear medium, that is, it is the sum of the amplitudes of the two applied fields and of any fields generated by the transverse instability.

Figure 3(a) shows numerical results obtained by numerically solving Eq. (1) using a split-step Fourier method[16] for three situations at relatively low pumping intensities. At the lowest intensity, the beams are essentially unaffected by the interaction. At a slightly higher intensity, whole-beam self-focusing of each beam begins to be observable, but interaction of the beams is still not present. At still higher intensities, the individual pump beams undergo significant whole-beam self-focusing and small-scale filamentation, and two-beam-excited self-diffraction spots can be seen. By increasing the intensity yet further to match the experimental conditions of Fig. 2, the results in Fig. 3(b) are obtained. Now, two self-diffraction orders are clearly visible on either side of the pump beams. Also, the pump beams show serious degradation due to filamentation.

Because of saturation of the response of the camera, it is not possible to make a quantitative comparison between the results of Figs. 2 and 3(b). Instead, we performed separate measurements of the energy of each of the spots shown in Fig. 2. We find that the fractions of the pump energy contained in the first three orders of diffraction are given by 0.16, 0.04, and 0.005. It can be seen that the results of the simulation shown in Fig. 3(b) are in very good agreement with these measured values. Slightly more than 50% of the energy was lost into high-order filamentation modes (the halo around the pump beams), and much

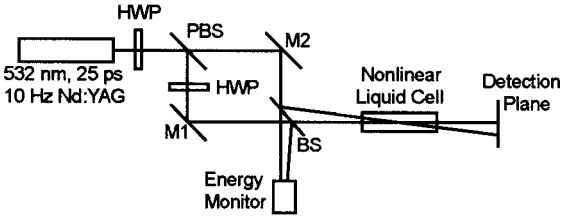

Fig. 1. Experimental setup. M1, M2, mirrors. Other abbreviations defined in text.

0146-9592/06/070951-3/$15.00

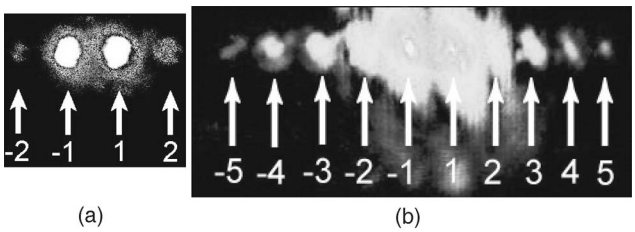

Fig. 2. Experimentally observed self-diffraction pattern generated by crossing two intense laser beams in CS_2 at a crossing angle of 3.2 mrad. (a) Normal exposure to see defined pump beams with the first side modes barely visible. (b) Overexposed to make the high-order components visible.

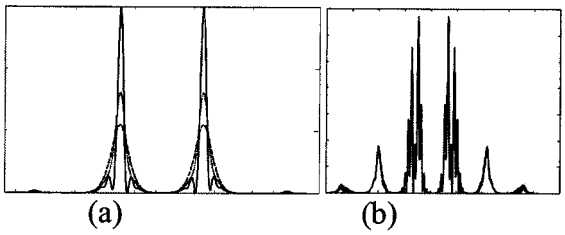

Fig. 3. Numerical simulations of the self-diffraction experiment for a 10 cm CS_2 cell and a 3.2 mrad crossing angle. Several pumping conditions are shown: (a) 2.8, 5.7, and 8.6 MW/cm^2. Note the beginning of the growth of side modes for the highest intensity. (b) 11.3 MW/cm^2, matching the conditions of Fig. 2.

less than 1% of the energy was contained in the higher-order ($|N|>3$) diffraction orders.

At larger crossing angles (greater than approximately 5 mrad), an array of spots is no longer seen, but instead the pattern takes on a ring structure. Two distinct types of conical emissions were observed. In the first type, a cone is formed between the two pump beams. The mechanism for this process, known as TBECE is well understood.[13] Figure 4 shows a TBECE pattern obtained in the experiment. An additional interesting feature is the bright spot in the center of the cone. The phase matching condition required for the generation of the bright spot is exactly the same as that for filamentation,[17] but now with the off-axis modes acting as the pump and the central spot growing from noise.

In the second type of conical emission, two large cones are generated. Each cone passes through one of the pump beams and is approximately centered on the other beam. We believe that this process is a form of seeded modulational instability (SMI). In this process, one of the applied beams acts as a pump and the other acts as a seed to initiate the process. TBECE requires that the energy of the pump beams be nearly equal,[11] but it can occur at relatively low intensities; SMI can occur with unbalanced pumping but requires higher intensities to form. Thus, these processes can occur either independently or simultaneously, depending on pumping conditions. Figure 5 shows a case in which both TBECE and SMI occur simultaneously, with the accompanying diagram showing the key features of the pattern.

We have identified a clear threshold for the occurrence of SMI. In determining this threshold, we varied the input parameters to determine that the threshold condition depends only on the total nonlinear phase shift acquired by the pump beam. Three nonlinear liquids, carbon disulfide (CS_2), carbon tetrachloride (CCl_4), and toluene (C_7H_8) (each with different values of n_2), were used. Both a 3 and a 10 cm cell and two different beam waist sizes were used. In all cases, it was found that the threshold for visually noticeable SMI was approximately 0.19 rad of nonlinear phase in the pump beam. In comparison, the cones shown in Fig. 5 were generated from a configuration yielding 0.75 rad of nonlinear phase for each pump, which is well above threshold.

To explore the origin of the SMI process, we have performed a series of measurements in which we vary the relative strength of the two pump beams. Figure 6(a) shows a case in which the two pump beams carry significantly different power. The strong (right) beam would (in the absence of the other beam) produce 0.75 rad of nonlinear phase shift, whereas the weak beam would (in the absence of the other beam) produce 0.15 rad of nonlinear phase shift. Since the weak beam is below the SMI threshold, it does not generate a noticeable cone. However, the strong beam nonetheless creates a cone that is seeded by the presence of the weaker beam. We have determined that the properties of the cone are nearly independent of the strength of the seed. Figure 6(b) shows the results when one of the beams is completely blocked. We see that no cone is produced in this case; only a single-beam filamentation halo sur-

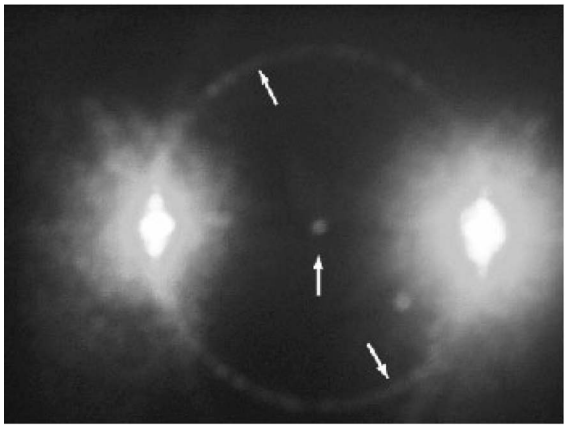

Fig. 4. TBECE in CS_2. Note the bright spot at the center of the cone, which is formed by the inverse of the usual filamentation process. The two other arrows point to diametrically opposite regions of the cone; photons at these two points are expected to be entangled.

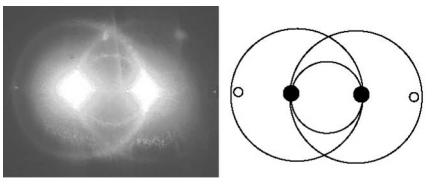

Fig. 5. Simultaneous presence of TBECE (small circle) and SMI (large circles) in CS_2. Note also the bright spots opposite the pump beams (showing that lowest-order self-diffraction is also present). The drawing shows the key features of the pattern.

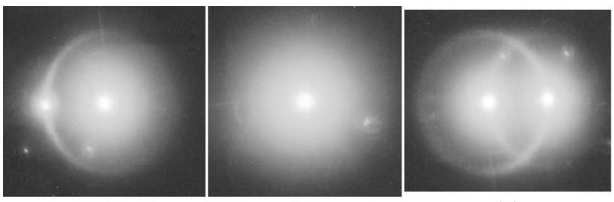

Fig. 6. Seeded conical modulational instability in CS_2. (a) Attenuated (left) beam contains 20% of the intensity of the strong beam; strong is well above threshold, weak is just below. (b) One beam completely blocked. (c) Both beams of nearly equal intensity, resulting in two cones.

rounding the pump beam is seen. Figure 6(c) shows the case of two beams of nearly equal intensity, and the pattern has the form of a cone surrounding each pump beam. The results of Fig. 6 support the interpretation that SMI occurs because one input beam acts as a pump and the other input acts as a seed that triggers the instability.

We have also determined that, while the intensity of the cone is determined primarily by the intensity of the pump beam (the beam about which the cone is formed), essentially all the other properties of the cone, such as its polarization, depend on the properties of the seed. The fact that the polarizations of the cones will follow the polarizations of the seeds gives us reason to believe that this process could be a candidate for a source of polarization-entangled photons.

It should be noted that, in the case of unseeded modulational instability (which was not witnessed in this study as small-scale filamentation due to pump beam quality depleted the single-beam energy needed to initiate that process), the generated mode grows in a cone about the pump at the angle of maximal gain associated with single-beam filamentation. However, in the case of seeded modulational instability, if the seed intensity is a significant fraction compared with the pump intensity, not only does the angle of maximal growth match the seeding angle but also the form of the output can change significantly.

In summary, we have identified several forms of pattern formation that can occur when two laser beams intersect in a nonlinear optical liquid. The observations are in good agreement with theoretical interpretations. It is hoped that these processes can be used in the development of new nonlinear sources of light, including those of use in studies of quantum information processing.

We thank Elizabeth Hill for her assistance in collecting some of the data reported here. This work was supported by the U.S. Army Research Office.

*Present address, Department of Physics, Adelphi University, Garden City, New York 11530; e-mail address, bentley@adelphi.edu.

†Present address, Lawrence Livermore National Laboratory, Livermore, California.

References

1. T. Yajima and H. Souma, Phys. Rev. A **17**, 309 (1978).
2. C. V. Heer and N. C. Griffen, Opt. Lett. **4**, 239 (1979).
3. A. Von Jena and H. E. Lessing, Opt. Quantum Electron. **11**, 419 (1979).
4. L. J. Rothberg and N. Bloembergen, Phys. Rev. A **30**, 2327 (1984).
5. C. J. McKinstrie and R. Bingham, Phys. Fluids B **1**, 230 (1989).
6. C. J. McKinstrie and R. Bingham, Phys. Fluids B **2**, 3215 (1990), erratum of Ref. 5.
7. G. G. Luther and C. J. McKinstrie, J. Opt. Soc. Am. B **7**, 1125 (1990).
8. D. J. Harter, P. Narum, M. G. Raymer, and R. W. Boyd, Phys. Rev. Lett. **46**, 1192 (1981).
9. D. J. Harter and R. W. Boyd, Appl. Phys. B: Photophys. Laser Chem. **29**, 163 (1982).
10. E. K. Kirilenko, S. A. Lesnik, V. B. Markov, and A. I. Khyzniak, Opt. Commun. **60**, 9 (1986).
11. M. Kauranen, J. J. Maki, A. L. Gaeta, and R. W. Boyd, Opt. Lett. **16**, 943 (1991).
12. M. Kauranen, A. L. Gaeta, and C. J. McKinstrie, J. Opt. Soc. Am. B **10**, 2298 (1993).
13. W. Chalupczak, W. Gawlik, and J. Zachorowski, Opt. Commun. **111**, 613 (1994).
14. R. S. Bennink, V. Wong, A. M. Marino, D. L. Aronstein, R. W. Boyd, C. R. Stroud, Jr., S. Lukishova, and D. J. Gauthier, Phys. Rev. Lett. **88**, 113901 (2002).
15. R. W. Boyd, *Nonlinear Optics*, 2nd ed. (Academic, 2002).
16. G. P. Agrawal, *Nonlinear Fiber Optics* (Academic, 1989).
17. V. I. Bespalov and V. I. Talanov, Sov. Phys. JETP **3**, 307 (1966).